scientific reports

Check for updates

OPEN

Mycorrhizal symbiosis between *Coprinellus disseminatus* and *Cremastra appendiculata*, insights from gene expression

Lei Huang[2] & Yanyan Gao[1]✉

Orchid seed germination is an extremely complex physiological and ecological process that includes seed development and mutualistic interactions with compatible mycorrhizal fungi. Although the mycobiont *Coprinellus disseminatus* associated with *Cremastra appendiculata* has been reported, the mutualistic interactions between them remain poorly understood. In this study, we performed physiological and transcriptomic analyses to compare symbiotic germination and ungerminated seeds of *Cr. appendiculata*, as well as free-living *Co. disseminatus*, to investigate changes in physicochemical content and identify key genes that regulate the symbiotic germination of *Cr. appendiculata* seeds. The results revealed the content of auxin (IAA), gibberellic acid (GA_3), salicylic acid (SA) and jasmonic acid (JA) of *Cr. appendiculata* protocorms increased during symbiotic germination, and the content of superoxide dismutase (SOD) and catalase (CAT) in the symbiotically germinating protocorms also higher than ungerminated seeds. However, the content of peroxidases (POD) showed lower in the symbiotically germinating protocorms than ungerminated seeds. A total of 5,913 genes showing different levels of expression (log_2FPKM ≥ 2.0, FDR < 0.01) in the comparison of CA and SY, and 19,077 differentially expressed genes (DEGs) genes in the comparison of CD and SY. DEGs involved in carbon metabolism, lipid metabolism, plant defense, plant hormone signal transduction and biotin metabolism were identified with significant upregulation or downregulation of genes related to metabolism observed. This work provides that mycorrhizal fungus *Co. disseminatus* can increase the content of endogenous hormones to promote *Cr. appendiculata* seed germination, and change the content of SOD, CAT to protect the plant against oxidative damage. These data may contribute to a better understanding of the molecular mechanisms of symbiotic germination and mycorrhizal fungi interactions.

Keywords Orchid, Mycorrhizal interaction, Seed germination, Transcriptome

Abbreviations

Cr. appendiculata	Cremastra appendiculata
Co. disseminatus DJF-10	Coprinellus disseminatus DJF-10
OMA	Oatmeal agar medium
CA	*Cremastra appendiculata* asymbiotically ungerminated seeds at 25 days after sowing
SY	*Cremastra appendiculata* symbiotic germinated seeds at 25 days after sowing
CD	Free-living mycelium of *Co. disseminatus* DJF-10 grown on the OMA medium
DEG	Differentially expressed genes
NR	Non-redundant proteins
KEGG	Kyoto encyclopedia of genes and genomes
GO	Gene ontology
FPKM	Fragments per kilobase per million mapped reads
FC	Fold change
ABA	Abscisic acid
IAA	Auxin

[1]Guizhou Medical University, Guiyang 550025, Guizhou, People's Republic of China. [2]Guizhou Academy of Forestry, Guiyang 550025, Guizhou, People's Republic of China. ✉email: yygaoluck@163.com

GA	Gibberellic acid
SA	Salicylic acid
JA	Jasmonic acid
POD	Peroxidases
SOD	Superoxide dismutase
CAT	Catalase

The Orchidaceae family is the most species-rich in the plant kingdom boasting over 28,000 identified species[1]. Owing to their significant ornamental and medicinal value, many of these species are facing severe extinction risks, highlighting an urgent need for conservation[2]. Symbiotic seed germination plays a crucial role in orchid propagation and reintroduction, serving as a vital strategy for conserving orchid species in their natural habitats. While significant progress has been made in understanding the diversity and specificity of orchid mycorrhizal fungi, as well as the morphological changes in host cells and mycobionts during symbiotic germination[3–6], the physiological and molecular processes induced by mycorrhizal fungi during symbiotic germination are still largely unknown.

Orchid seeds are minuscule, dust-like, with a lignified seed coat, and they rely heavily on compatible mycorrhizal fungi for carbohydrates nutrients[7–9]. The symbiotic relationship between fungi and orchids encompasses three typical stages: hyphal invasion, colonization and mycelial coil formation, followed by mycelial digestion and degradation[10]. During the symbiosis, a series of physiological dynamic changes undergoes. The host and the invading hyphae form defensive and counter-defensive mechanisms, finally reaching a balanced and stable state. In this process, endogenous hormones play an irreplaceable role[11]. Additionally, due to the small amount of energy stored in orchid seeds. It has been observed that the host obtains nutrients such as carbon and nitrogen for embryonic development by degrading living pelotons or the degradation of intercellular hyphae[3,5,12,13]. It is still unclear how to metabolize and transform material energy during the symbiosis between plants and fungi. Therefore, it is of great significance to explore the changes in physiological indices in the symbiosis process between orchids and fungi in a timely manner to deeply explore the symbiosis mechanism.

Recent studies on orchid symbiosis have shed light on the mechanism of symbiotic germination through molecular biology approaches, including high-throughput sequencing[4,14]. For instance, research reported that symbiotic germination appeared to induce higher expression of some genes and proteins in lipid carbohydrate metabolism, the antioxidant activity in plants during the symbiotic germination of *Dendrobium officinalis*[15], which provided new insights into the molecular basis of orchid seed germination, as revealed through transcriptomic and proteomic analyses. Miura et al.[4] investigated the orchid-mycorrhizal symbiosis by analyzing the transcriptome of *Bletilla striata* associated with *Tulasnella sp.* at an early development stage, suggesting that essential genes for a mutualistic relationship with arbuscular mycorrhizal (AM) fungi were expressed in *Bl. striata*. Furthermore, genes related to plant defense, such as nodulin-like and Ca^{2+} signal transduction pathways, have been upregulated in protocorms during symbiotic germination of orchid seeds and fungi[4,16,17]. These insights provide valuable information for further investigation into the interaction mechanisms between mycorrhizal fungi and orchids.

Cremastra appendiculata, a member of the orchid family, is found across Japan, Taiwan, Korea, and other regions of Eastern Asia[18]. Our previous studies have highlighted the role of its mycorrhizal fungus, *Coprinellus disseminatus* in promoting the germination of *Cr. appendiculata* seeds by successfully breaking down the lignified seed coat during the symbiotic germination[5,14]. Despite this advancement, the specific interaction mechanisms between *Cr. appendiculata* and *Co. disseminatus* remain unclear, posing challenges to the cultivation of *Cr. appendiculata* seeds with its functional fungus. The germination of orchid seeds under natural conditions involves a complex and unique sequences of physiological and biochemical processes, including colonization, degradation of the lignified seed coat, lipid degradation, stimulation of plant growth and plant's response to the fungus[17]. Understanding the metabolic processes and gene expression at various stages of symbiotic germination is crucial.

To delve deeper into the molecular aspects of symbiotic germination of orchid seeds, we analyzed the physicochemical contents of symbiotic protocorms and ungerminated seeds of *Cr. appendiculata*. We then conducted a comparative transcriptomic analysis between seeds germinated symbiotically and ungerminated asymbiotically. This approach aims to uncover new insights into the biosynthesis and metabolism of carbon and lipid, as well as plant hormone signal transduction during the germination process.

Materials and methods

Experimental materials and growth conditions

In this study, we utilized the *Coprinellus disseminatus* DJF-10 and *Cremastra appendiculata* seeds as our experimental materials. The *Co. disseminatus* DJF-10 fungus was originally isolated from the roots of wild *Cr. appendiculata* plants, as reported in our previous research[6]. The seeds of *Cr. appendiculata* for germination were collected from different plants growing on farmland in Guiyang, Guizhou Province, PR China. All flowers were hand-pollinated by us in April to May, and seeds matured in October. Seeds were sterilized with 75% ethanol (30 s) and 1% sodium hypochlorite solution (3 min), and finally rinsed with sterile distilled water five times[6]. After surface sterilization, the seeds were divided into two groups. The first group of seeds was co-cultured with *Co. disseminatus* DJF-10 on oatmeal agar (OMA) medium (4 g L^{-1} milled oats, 8 g L^{-1} agar, pH of nature) to promote symbiotic germination (SY) with a germination rate of 68.45 ± 1.27% after sowing 25 days (Fig. 1a), while the second group was cultured on the same medium without the fungus to serve as the asymbiotic control (Fig. 1b). Conversely, the asymbiotic group's seeds did not germinate, and these were designated as the asymbiotic seeds group (CA). Additionally, free-living mycelium of *Co. disseminatus* DJF-10 grown on the OMA medium was defined as the CD group. All experimental setups were cultured and maintained in a growth

Fig. 1. Seeds of *Cr. appendiculata* in asymbiotic and symbiotic germination. (**a**) Seeds symbiotically germinated after 25 days. (**b**) Seeds asymbiotically ungerminated after 25 days. (**c**) A symbiotic protocorm with Trypan blue staining. Arrows indicate pelotons.

chamber at a constant temperature of 22 ± 2 °C in complete darkness, in line with protocols established in previous study[6]. Samples from the SY, CA, and CD groups were collected 25 days post- sowing. Seeds in the symbiotic germination group developed into protocorms, with microscopic observations revealing intracellular hyphae penetration and colonization by the fungus (Fig. 1c). The collected samples were immediately frozen in liquid nitrogen and stored at − 80 °C for subsequent biochemical analyses and RNA extraction. Three biological replicates were prepared for each biochemical and transcriptome analysis.

Determination of endogenous hormones during germination of *Cr. appendiculata*

The determination of auxin (IAA), gibberellic acid (GA_3), and salicylic acid (SA) content referred to the methods with slight modification[2,19]. The specific operation steps were as follows: a 0.1 g sample was weighed, the tissue was extracted at 4 °C overnight by 1.5 mL of pre-cooled 80% methanol aqueous (IAA and GA_3) or 90% methanol (SA) solution. It was centrifuged at 8000 *rpm* for 10 min, and the supernatant was collected to a new tube and dried with nitrogen. Then, 0.2 mL of mobile phase was added to dissolve it, mixed well, and stored at a low temperature for use. And the extract was filtered through a 0.45 μm organic microporous membrane and determined using the HPLC (Agilent1100) external standard curve method with a wavelength set at 254 nm for GA_3 and IAA, and at 302 nm for SA. The extraction and fractionation of jasmonic acid (JA) were conducted according to the method[17]. The tissue was extracted overnight at 4 °C in 1.5 mL of 80% methanol. After centrifugation at 8,000 *rpm* for 10 min, the supernatant was collected in a new tube. This eluate was then evaporated and resuspended in 0.2 mL of 0.1% phosphate-buffered saline (PBS) in acetonitrile (v: v = 55:45), filtered through spin columns, and subjected to HPLC (Waters 2695, USA) analysis with a wavelength set at 210 nm.

Determination of peroxidases (POD), superoxide dismutase (SOD) and catalase (CAT) of *Cr. appendiculata*

The activity of POD was measured utilizing a UV spectrophotometer employing the method with necessary modifications[20]. Samples (1.0 g) were pulverized in liquid nitrogen and homogenized in 4 mL of sodium phosphate buffer (200 mM, pH 6.8), followed by centrifugation at 8000 *rpm* at 4 °C for 10 min. The resultant supernatant was mixed with 1 mL of 50 mM PBS buffer, 200 μL of 10 mM hydrogen peroxide (H_2O_2), 3 mL of 25 mM guaiacol, and 1 mL of enzyme extract. POD activity was quantified relative to dry weight, reported as U g^{-1} protein. The contents of SOD and CAT were assessed using commercial SOD and CAT assay kits (Suzhoukeming Biotech, China), following the manufacturer's instructions.

RNA extraction, library construction and de Novo assembly

Total RNA was isolated from 100 mg of sample material using an RNA extraction Kit (Omega Bio-Tek, USA), in accordance with the manufacture's protocol. The extracted RNA was treated with RNase-free DNase I to eliminate any genomic DNA contamination. The purity and concentration of the RNA were verified using a NanoDrop One spectrophotometer (Nanodrop Technologies Inc., CA, USA), while the Agilent 2100 Bioanalyzer (Agilent Technologies, Santa Clara, CA, U.S.A.) was utilized to assess RNA concentration and integrity, and 1% agarose gel electrophoresis was conducted to check for RNA degradation and contamination. The library construction and sequencing were carried out on an Illumina HiSeq4000 platform (Illumina Inc., CA, USA) by the Beijing Genomics Institute (Shenzhen, China). The total clean reads were derived by elimitationg reads containing adapters, ambiguous sequences ($N > 5\%$), and low-quality reads (greater than 20% of bases in a read with a quality value $Q \leq 15$) from the initial raw data. And de novo assembly of the clean reads was performed to construct transcripts using Trinity version V2.0.6 for the assembly process. The assembled transcripts were further aligned using the Bowtie2 version 2.2.5 program, utilizing default parameters for accuracy[21].

Functional annotation of unigenes, and differentially expressed genes (DEG) analysis

Unfortunately, reference genomes of *Cr. appendiculata* and *Co. disseminatus* DJF-10 have not been published yet. It was technically unable to exclude the fungal involvement in the symbiotic seeds. Therefore, the fungal *Co. disseminatus* DJF-10 de novo group was assembled individually using trinity at default parametes. The coding sequences of symbiotic protocorms were mapped to the fungal de novo assembly nonredundant protein database. Then, all the mapped *Co. disseminatus* DJF-10 reads were removed from the symbiotic group using

Bowtie program[22,23], and the remaining unpaired reads were classified as the de novo reference assembly of *Cr. appendiculata*. The structure of mRNA sequences was much different from *Cr. appendiculata* and *Co. disseminatus* DJF-10. Therefore, we have removed the unigenes that were not annotated with plants as references. Lastly, the remaining unigenes were used for functional analysis, and were prepared to detect the gene expression levels between CA and SY. Also, we used the same method to remove *Cr. appendiucalata* reads from the symbiotic group (SY), and the remaining unpaired reads were annotated with fungal reads in the SY group, and used for functional analysis between the comparison of CD and SY.

Fold change (FC) denotes the ratio of gene expression levels between different groups with positive values indicating upregulation and negative values indicating downregulation of genes in the SY group compared to the control. Additionally, gene expression was quantified using fragments per kilobase of transcript per million mapped reads (FPKM) to ensure precise measurement. To predict functions and obtain functional descriptions of unknown genes, all assembled unigenes were aligned against the National Center for Biotechnology Information (NCBI) database using BLASTx. The complete series of fungal and plant transcriptomic data have been deposited in the NCBI database (accession No. PRJNA1065130). Additionally, several genes related to endogenous hormones in the symbiotic germination of *Cr. appendiculata* were selected for confirmation of their expression by qRT-PCR. Briefly, 1 μg of RNA was reverse-transcribed to cDNA using a reverse transcription system. The *CaEF-1α* gene and *CaRPS4* gene were used as the reference genes. The thermal cycle protocol used for qRT-PCR was 95 °C for 30 s, then 35 cycles of 95 °C for 5 s, finally 60 °C for 30 s. The relative gene expression was calculated using the $2^{-\Delta\Delta Ct}$ method. The primer sequences are listed on Table S1. The results of qRT-PCR and DEG are shown as a fold change of gene expression relative to the control sample.

Statistical analysis

Data from different samples were analyzed using analysis of student's test (t-test). The means were differentiated using t-test (least significant difference at $p < 0.05$) to perform all pairwise comparisons among different samples. Statistical analyses were conducted using SPSS Statistics software, version 25.0.

Results

Assays of IAA, GA_3, JA, and SA content

Endogenous hormones not only play an important role in seed germination but also play an irreplaceable role in plant-microbial interactions. To explore the changes in the content of endogenous hormones during the germination of *Cr. appendiculata* seeds, HPLC was used to quantify the four types of endogenous hormones: IAA, GA_3, JA, and SA. The IAA content in the ungerminated seed (CA) sample was low, only 0.45 μg g^{-1}. And its content reached 2.35 μg g^{-1} under symbiotic germinated seeds (SY), which was 5.4 times higher than CA ($p<0.05$) (Fig. 2a). The GA_3 content of mature seeds was 8.35 μg g^{-1}, and when the seed symbiotic with fungus and developed into a symbiotic protocorm, its content increased to 9.34 μg g^{-1}, which was higher than ungerminated seeds ($p<0.05$) (Fig. 2b). JA levels were high in ungerminated seeds (1.68 μg g^{-1}) and continued to increase during symbiotic germination ($p<0.05$) (Fig. 2c). Conversely, only minute amounts of SA (0.011 μg g^{-1}) were detected in ungerminated seeds, but SA levels dramatically increased during symbiosis at the protocorm stage ($p<0.05$) (Fig. 2d). These findings demonstrate that invasion of *Cr. appendiculata* seeds by the fungus may triggers a plant hormone response, facilitating seed germination.

Assays of POD, SOD and CAT content

We measured the activities of POD, SOD and CAT in both symbiotic protocorms and ungerminated seeds of *Cr. appendiculata* to investigate their roles in protecting the plant against oxidative damage. The results revealed lower POD activity in the symbiotic protocorms compared to ungerminated seeds (Fig. 3), which may beneficial for mycelium invading. However, the activities of SOD and CAT were significantly higher in the protocorms ($p < 0.05$), aligning with gene expression related to plant defense. These findings suggest that *Co. disseminatus* DJF-10 may confer protection to *Cr. appendiculata* against oxidative damage during their interaction.

Global analysis of the transcriptomic data and identification of core plant gene expression

To explore the transcriptome of *Cr. appendiculata* and its endosymbiont *Co. disseminatus* DJF-10 with improved sequence coverage, nine cDNA libraries were generated from RNA extracted from SY, CA, and CD. Quality assessment revealed Q30 values exceeding 87%, indicating the high-quality of reads suitable for subsequent analyses (Table S1). A total of 5,913 genes ($|\log2FC| \geq 2.0$, FDR < 0.01) were identified as DEGs during the symbiotic germination stage (SY) compared to ungerminated seeds (CA) (Fig. 4a). Among these DEGs, 2,773 were up-regulated, and 3,140 were down-regulated. Further analysis of gene expression between the symbiotic germination stage of SY and CD revealed 19,077 DEGs, with 17,388 up-regulated and 1,689 down-regulated in the symbiotic group (Fig. 4b).

GO (gene ontology) and KEGG (Kyoto encyclopedia of genes and genomes) enrichment analysis

To investigate the differences in metabolic processes between the symbiotically germinated seeds and the asymbiotically ungerminated seeds, GO analysis was conducted for the DEGs. Among the GO terms of DEGs, catalytic activity, binding, cell, membrane, cell, membrane part, cellular process and metabolic process terms were significantly overrepresented in comparison between CA and SY, and between CD and SY (Fig. 5). In particular, the terms related to antioxidant activity and nutrient reservoir activity were also found in comparison between CA and SY.

Also, KEGG pathway annotation results indicated that the comparison between CA and SY involves various biological pathways, including phenylpropanoid biosynthesis, carbon metabolism, starch and sucrose

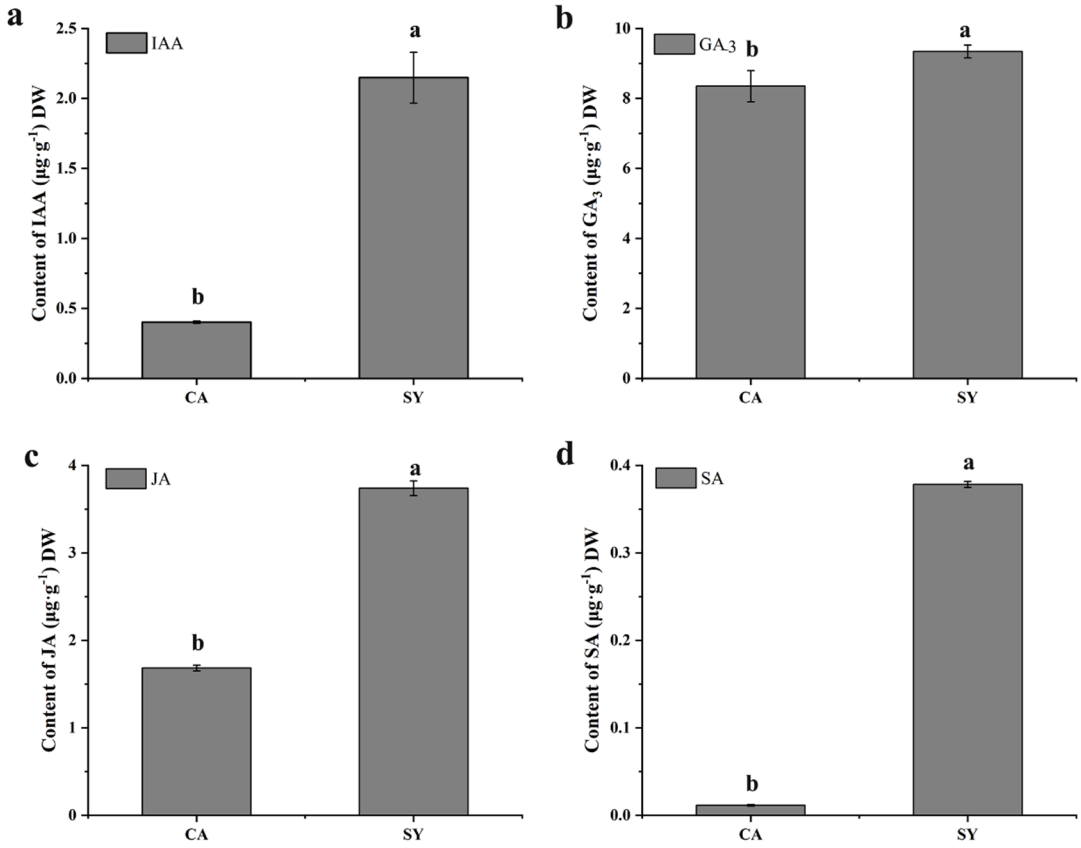

Fig. 2. Changes of endogenous hormone content at symbiotic protocorm and ungerminated seeds of *Cr. appendiculata*. (**a**) Content of IAA. (**b**) Content of GA_3. (**c**) Content of JA. (**d**) Content of SA. Different letters indicated a significant difference between the treaments (p<0.05). The same below.

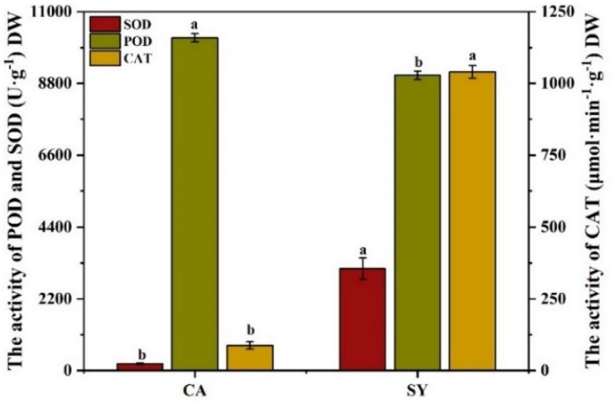

Fig. 3. Changes of enzymes in symbiotic germinated and ungerminated seeds of *Cr. appendiculata*.

metabolism, pentose and glucuronate interconversions, amino sugar and nucleotide sugar metabolism, plant-pathogen interaction, plant hormone signal transduction, and MAPK signaling pathway–plant (Fig. 6a) (Tab. S2). Notably, in the comparison between CD and SY, several pathways were distinctly enriched, including those related to endocytosis, MAPK signaling pathway–yeast, biosynthesis of antibiotics, amino sugar and nucleotide sugar metabolism, carbon metabolism, biosynthesis of amino acids, purine metabolism, starch and sucrose metabolism (Fig. 6b). Below, we provide a comprehensive functional interpretation of how these DEGs may contribute to the process of symbiotic germination.

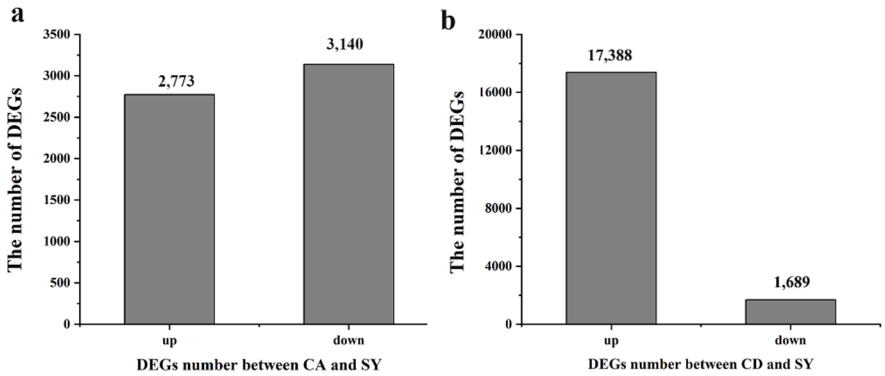

Fig. 4. Statistical analysis of the annotated and differentially expression unigenes. (**a**) DEGs number between CA and SY. (**b**) DEGs number between CD and SY.

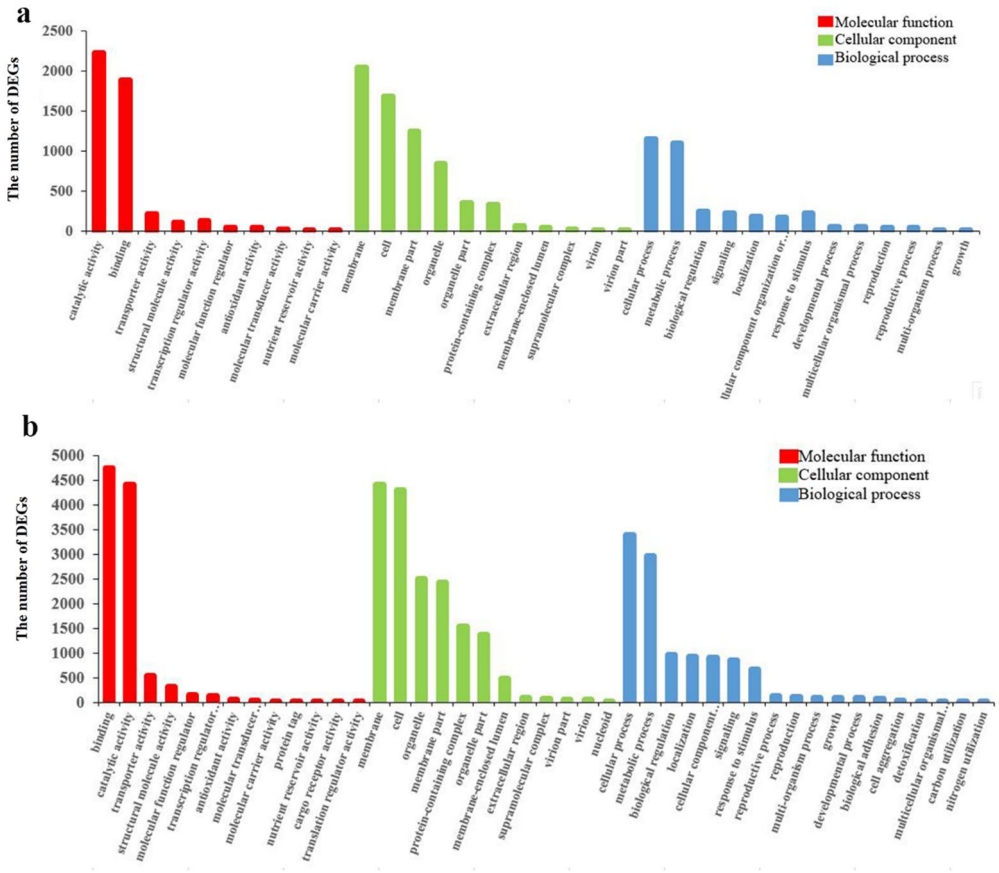

Fig. 5. Significantly overrepresented GO terms in the symbiotic germination. (**a**) GO classification between CA and SY. (**b**) GO classification between CD and SY.

Carbohydrate metabolism in symbiotic germination of *Cr. appendiculata*

In our transcriptomic analysis, the pathway of carbohydrate metabolism was significantly enriched. In addition, starch and sucrose metabolism, pentose and glucuronate interconversions, as well as glycolysis/gluconeogenesis, were enriched in the upregulated DEGs in CA compared to SY. We discovered that 263 genes associated with carbon metabolism exhibited an upregulation ranging from 2.0- to 9.9-fold and 189 genes down-regulation in the comparison between CA and SY. Additionally, 57 genes related to pentose and glucuronate interconversions displayed up-regulated and 39 genes displayed down-regulated. In addition, 30 genes associated with glycolysis/gluconeogenesis were up-regulated and 32 genes were down-regulated. Furthermore, 86 genes linked to starch and sucrose metabolism were upregulated showing 2.0- to 8.7-fold changes in expression and 44 genes were down-regulated at the protocorm stage in comparison between CA and SY (Table 1). Therefore, it appears that

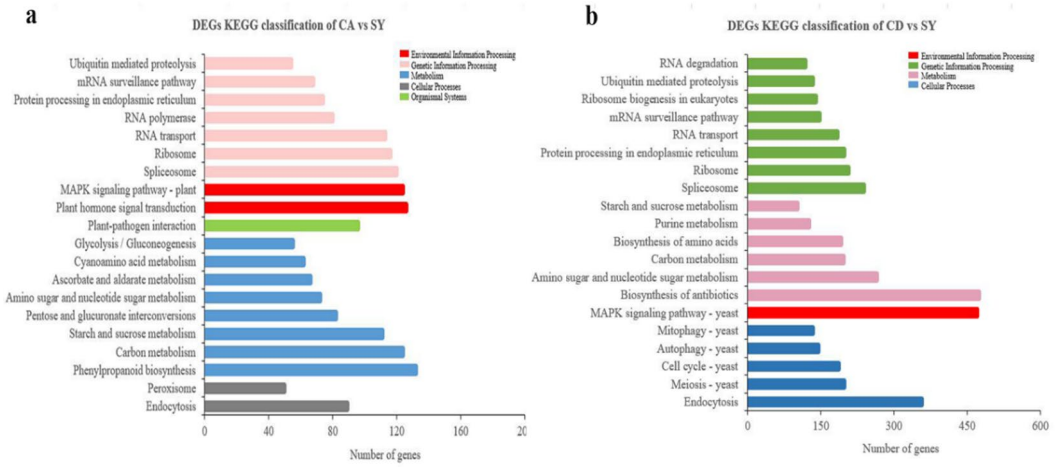

Fig. 6. Significantly overrepresented KEGGS pathways in the symbiotic germination. (**a**) KEGG pathways enrichment between CA and SY. (**b**) KEGG pathways enrichment between CD and SY.

glycolysis and the Calvin cycle could be involved in the carbohydrate metabolism observed in the protocorm following fungal inoculation.

Lipid metabolism in *Cr. appendiculata*

Orchid seeds are known to contain substantial concentrations of lipid reserves, which degrade slowly during seed germination[24]. Our RNA-seq transcriptomic analysis of *Cr. appendiculata* seeds inoculated with *Co. disseminatus* DJF-10 revealed that pathways related to fatty acid elongation and degradation were enriched during the symbiotic germination process. We identified several genes upregulated in these metabolic pathways (Tab.S3). Specifically, 21 genes associated with fatty acid degradation were upregulated in the SY protocorm by more than a 2-fold change compared to ungerminated seeds (Fig. 7a). Additionally, nine genes associated with fatty acid biosynthesis were upregulated and 12 genes were downregulated, while the gene encoding acetyl-CoA carboxylase biotin carboxyl carrier protein (BCCP) (unigene45942_All) showed increased expressing at the protocorm stage (8.2-fold change) in *Cr. appendiculata* (Fig. 7a). BCCP is a component of acetyl-CoA-carboxylase (*ACCase*), which catalyzes the conversion of acetyl-CoA to malonyl-CoA, a crucial step in the de novo biosynthesis of fatty acids[25]. This may suggest that fungal colonization promotes lipid degradation and its conversion into free fatty acids (FAAs), potentially serving as an energy source for seed germination. These findings leading us to guess that the degradation of stored lipids is a distinctive process in the symbiotic germination of seeds following fungal penetration.

Plant defense mechanisms in *Cr. appendiculata*

Our physiological analyses indicate elevated activities of CAT and SOD during fungal colonization, suggesting active plant defense responses (Fig. 3). Transcriptomic data revealed enrichment in phenylpropanoid biosynthesis and glutathione metabolism pathways when comparing between CA and SY conditions. Specially, 89 genes related to phenylpropanoid biosynthesis were up-regulated and 43 genes down-regulated at the protocorm stage in SY (Fig. 7b), aligning with findings in *Dendrobium officinale*[2]. Additionally, the expression levels of chitinase and basic endochitinase B, which are critical for defense against chitin-containing fungal pathogens, there were 21 genes increased in SY protocorms, showing 2.0-fold and 8.3-fold changes, respectively, compared to CA. Furthermore, 28 lectin genes, which are also indicators of plant defense were up-regulated in SY with fold changes exceeding two times (Fig. 7b). These results underscore the plant's regulatory response to fungal stimulation during *Cr. appendiculata* seed germination following fungal colonization.

Signal transduction in *Cr. appendiculata*

Plant hormones play crucial roles in plant-fungi interactions[2]. In our study, DEGs associated with hormone pathways were identified as follows. The genes encoding amidase (amiE) and aldehyde dehydrogenase (ALDH), which are associated with IAA synthesis through the tryptophan metabolism pathway, were up-regulated. The auxin transporter protein (AUX1) and auxin-responsive protein (AUX/IAA) genes were also up-regulated in the metabolic pathway in response to the increase in IAA synthesis (Fig. 8). Also, the genes encoding entcopalyl diphosphate synthase (CPS), entkaurene oxidase (KO), GA 20oxidase (GA20ox), GA 2oxidase (GA2ox) and GA 3beta dioxygenase (GA3ox) were upregulated in the symbiotic seeds. Those associated with the GID1, DELLA and TF were also upregulated. Accordingly, we speculate that the fungus may cause the changes of GA_3.

Furthermore, the expression levels of genes related to JA and SA also changed. The expression of lipoxygenase (*13sLOX*), hydroperoxide dehydratase (*AOS*), allene oxide cyclase (*AOC*) in SY were upregulated. It meant the biosynthesis of JA increased. At the same time, the genes expression of phenylalanine ammonialyase (*PAL*), cinnamate4hydroxylase (*C4H*), 4coumarateCoA lignase (*4CL*), nonexpressor of pathogenesis-related genes

Pathway	Gene ID	Log_2 CA/SY	Description
Carbohydrate metabolism	Unigene13238_All	2.27	Putative lipase ROG1
	Unigene40939_All	2.26	Hexokinase-3-like
	Unigene292_All	3.53	Glucan endo-1,3-beta-glucosidase 4-like
	Unigene46340_All	4.17	Predicted protein
	CL8834.Contig3_All	5.10	Glutamate dehydrogenase
	CL4362.Contig13_All	5.95	Formamidase
	Unigene3948_All	6.45	Glutathione dehydrogenase
	Unigene45942_All	8.24	Acetyl-CoA carboxylase biotin carboxyl carrier protein
	Unigene48170_All	5.58	Glutathione dehydrogenase
	Unigene48598_All	9.90	Glyceraldehyde 3-phosphate dehydrogenase
	CL8858.Contig2_All	9.11	Glyceraldehyde 3-phosphate dehydrogenase
	Unigene1805_All	− 5.71	Catalase isozyme 1-like
	CL1257.Contig1_All	− 5.04	Eukaryotic translation initiation factor 2 C
	Unigene34012_All	2.00	Glucan 1,3-beta-glucosidase A
	Unigene29591_All	2.35	Hypothetical protein
	Unigene19218_All	3.45	Lipase At1g29670-like
	Unigene11186_All	4.19	Beta-glucosidase 2
	CL9579.Contig3_All	5.45	Beta-glucosidase
	Unigene53556_All	5.59	Beta-glucosidase
Starch and sucrose metabolism	CL12990.Contig2_All	5.49	Alpha-trehalase
	CL817.Contig1_All	6.06	Beta-glucosidase
	CL817.Contig2_All	7.02	Beta-glucosidase
	CL3713.Contig1_All	7.10	Alpha-trehalase
	Unigene44669_All	8.48	Glucan endo-1,3-beta-glucosidase 4
	CL11005.Contig1_All	6.48	Beta-glucosidase
	Unigene10980_All	8.23	Beta-glucosidase
	Unigene8826_All	6.15	Glucan endo-1,3-beta-glucosidase 4
	Unigene3227_All	8.70	Beta-glucosidase
	CL3713.Contig7_All	5.02	Alpha-trehalase
	CL8595.Contig2_All	5.45	Trehalose 6-phosphate phosphatase
	CL2401.Contig2_All	6.88	E3 ubiquitin-protein ligase UBR4
	Unigene12438_All	5.83	Beta-glucosidase
	CL2401.Contig1_All	7.14	E3 ubiquitin-protein ligase UBR4
	Unigene5817_All	5.71	Beta-glucosidase
	CL5802.Contig2_All	− 8.29	Uncharacterized protein
	CL7846.Contig1_All	− 5.96	Beta-glucosidase
Pentose and glucuronate interconversions	Unigene45912_All	8.33	Peroxidase
	Unigene13610_All	8.15	Pectinesterase
	Unigene8085_All	7.24	Pectinesterase
	Unigene7618_All	5.61	Ubiquitin carboxyl-terminal hydrolase
	Unigene29133_All	5.38	Pectinesterase
	Unigene34936_All	5.30	Ormin 2
	Unigene33083_All	5.24	Pectinesterase
	Unigene12108_All	5.16	Pectinesterase
	Unigene11402_All	4.26	Polyprotein
	CL5124.Contig2_All	3.99	UDP-glucose 6-dehydrogenase 4-like
	CL7633.Contig4_All	2.35	Protein OSB2
	CL10814.Contig2_All	2.01	Pyrophosphorylase
	CL1083.Contig3_All	− 6.27	UDP-sugar pyrophosphorylase
	Unigene11031_All	− 5.89	Putative lipase
	CL2835.Contig15_All	− 4.90	Xylose isomerase isoform X1

Continued

Pathway	Gene ID	Log_2 CA/SY	Description
Glycolysis/ Gluconeogenesis	Unigene48598_All	9.90	Glyceraldehyde 3-phosphate dehydrogenase
	CL8858.Contig2_All	9.11	Glyceraldehyde 3-phosphate dehydrogenase
	Unigene3948_All	6.45	Glutathione dehydrogenase
	Unigene48170_All	5.58	Glutathione dehydrogenase
	Unigene10440_All	5.21	Alcohol dehydrogenase class-P
	Unigene45734_All	4.11	Aldehyde dehydrogenase 2B2
	Unigene864_All	3.73	Aldo-keto reductase family 4 member C9-like
	Unigene4339_All	3.05	Cytochrome P450 704C1-like
	Unigene15214_All	2.26	Aldose 1-epimerase
	Unigene35_All	− 5.06	Alcohol dehydrogenase 1-like
	CL2569.Contig3_All	− 4.51	Alcohol dehydrogenase 1
	Unigene14926_All	− 4.15	RNA pseudouridine synthase 1

Table 1. Part differentially expression plant genes involved in carbohydrate metabolism.

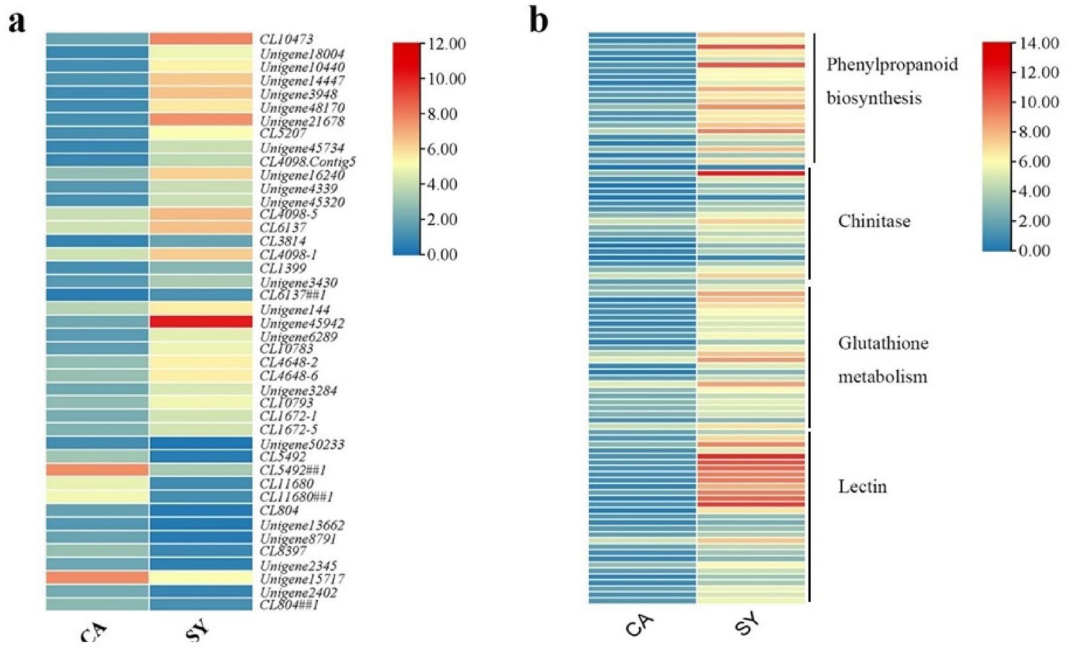

Fig. 7. Clustering of DEGs up-regulated of *Cr. appendiculata* during symbiotic germination. (**a**) DEGs related to lipid metabolism, (**b**) Part DEGs related to plant defense mechanism.

1 (*NPR1*), and transcriptome factor (TGA) in the phenylalanine metabolism were upregulated. It meant that symbiotic seed may obtain systemic acquired resistance.

Biotin metabolism in *Co. disseminatus*

Biotin, a water-soluble vitamin from the B complex, is an essential nutrient across organisms, from bacteria to host, serving as a cofactor for biotin-dependent carboxylases in crucial metabolic processes like gluconeogenesis, fatty acid synthesis, and amino acid catabolism[27]. For instance, the enzymes 3-oxoacyl-acyl-carrier protein reductase (FabC) plays a vital role in the fatty acid biosynthesis pathway. Our research found 19 genes related to biotin metabolism in the protocorm of *Co. disseminatus* DJF-10 following symbiosis with *Cr. appendiculata*, and all the genes up-regulated showing a 2.5-6.8-fold change (Fig. 9). This includes 13 genes encoding the catalyse enzymes (FabC) for fatty acid biosynthesis, two biotin ligases, three bifunctional enzymes, and one multifunctional beta-oxidation protein (Fig. 10). These findings suggest that *Co. disseminatus* DJF-10 penetration may enhance carbohydrate metabolism, potentially providing essential nutrients for the energy requirements of *Cr. appendiculata* seed germination.

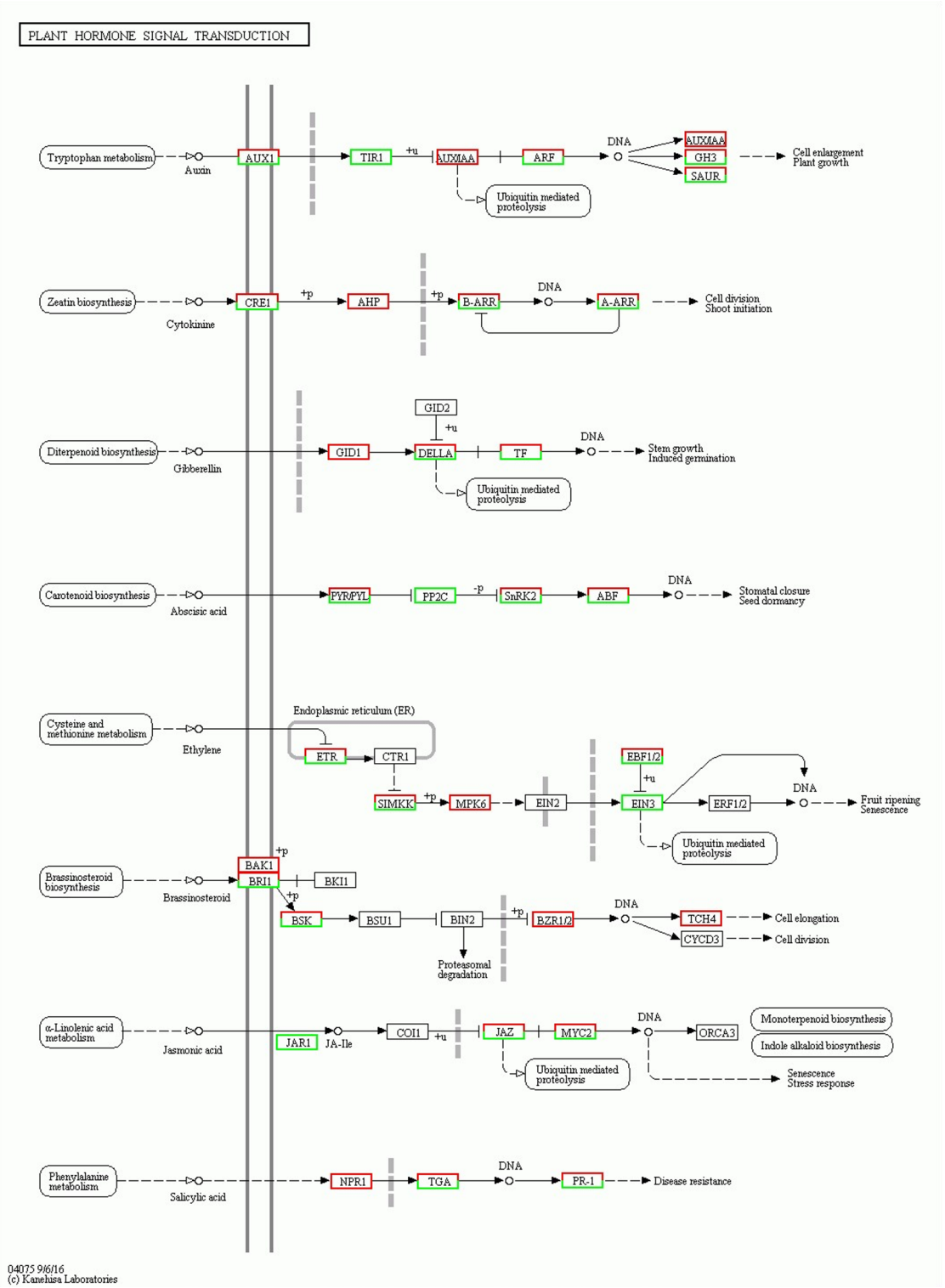

Fig. 8. The gene expression in the pathway of plant hormone signal transduction[26].

Verification of differential expression gene by qRT-PCR

To confirm findings of gene expression obtained from transcriptome data, 6 DEGs related to endogenous hormone biosynthesis were chosen for qRT-PCR (Fig. 11). The results showed that the genes had similar expression patterns to the content variations, which indicates the trustworthiness of the transcriptomic analysis.

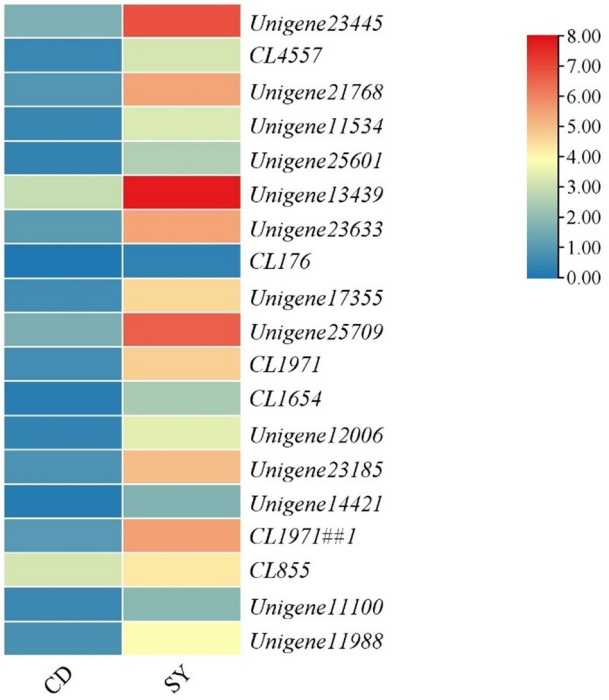

Fig. 9. Clustering of DEGs related to biotin mechanism of *Co. disseminatus* during symbiotic germination with *Cr. appendiculata*.

Discussion

The orchid *Cr. appendiculata* is among the species most challenging to propagate, with its mycorrhizal partner *Co. disseminatus* DJF-10, having been discussed in our prior work[6]. *Co. disseminatus* DJF-10 facilitates seed dormancy breakage through enzymatic action and enhances water uptake for the seed embryos[14]. However, the specifics of their interaction remain elusive, underscoring the need to explore the basis of these mechanisms further for potential large-scale cultivation.

In the context of seed germination, starch degradation in the endosperm is a critical process, supplying the primary energy and precursor molecules for anabolic reactions in many plants[15]. Yet, orchid seeds, characterized by their minuscule size and limited nutrient reserves, exhibit a distinct dependency. With mycorrhizal fungi, starch or cellulose becomes a key carbohydrate source initiating germination[7–9,28–30]. Our findings reveal the gene expression related to starch synthesis were upregulated during symbiotic germination. This result may suggest and upsurge in carbon metabolic activity diverging from the typical reliance on starch as energy reserve in the embryos. However, the guess still needs forward genetics. In contrast to species such as *Dendrobium officinale* and *Goodyera repens*, which utilize starch grains for nutrients storage in seed embryos[5,15], highlighting the diversity of nutrient storage strategies across orchid species.

Lipids serve as energy reserves in orchid seeds, with a notable surge in fatty acid levels in the protocorm stage of *Cr. appendiculata* (SY), suggesting lipid breakdown into fatty acids for metabolic energy use. This study further revealed that mature embryos possess significant lipid reserves. Upon *Co. disseminatus* DJF-10 mycelium invasion, an extensive upregulation of fatty acid-degrading enzyme genes occurred, contributing to fatty acid degradation (Fig. 7a). This process aligns with symbiotic structure observations and physiological and biochemical markers, indicating early-stage lipid metabolism during symbiotic germination of *Cr. appendiculata* seeds. The resulting acetyl-CoA enters the tricarboxylic acid cycle, fueling the synthesis of essential substances for embryonic development.

The germination process of seeds not only triggers the degradation of reserves, the generation of energy, and the synthesis of secondary metabolites but also activates the plant's antioxidant defense mechanisms in response to biotic or abiotic stress. Upon invasion by the symbiotic fungus, the activities of enzymes such as polyphenol oxidase, POD, CAT, and SOD significantly increase to protect the plant against oxidative damage, peaking when the hyphal coil decomposes[15,31]. Transitioning from dormancy to germination, seeds generate a substantial amount of reactive oxygen species (ROS), including hydroxyl radicals and hydrogen peroxide, leading to cellular damage. SOD plays a crucial role in scavenging superoxide anions (O_2-) by converting them into H_2O_2 and oxygen (O_2). Furthermore, CAT breaks down H_2O_2 into water and oxygen, thereby eliminating H_2O_2 from the cell and protecting it. POD works synergistically with CAT to remove H_2O_2, minimizing damage to cell membranes[32]. This study revealed that colonization by the mycelium of *Co. disseminatus* DJF-10 in the embryo of *Cr. appendiculata* led to the upregulation of several genes encoding antioxidant enzymes (SOD, POD, and CAT), corroborating the findings of *De. officinale*[15], and suggesting that the invasion by symbiotic orchid fungi may enhances the host's resistance to maintain internal environmental stability. Additionally, the phenylpropanoid

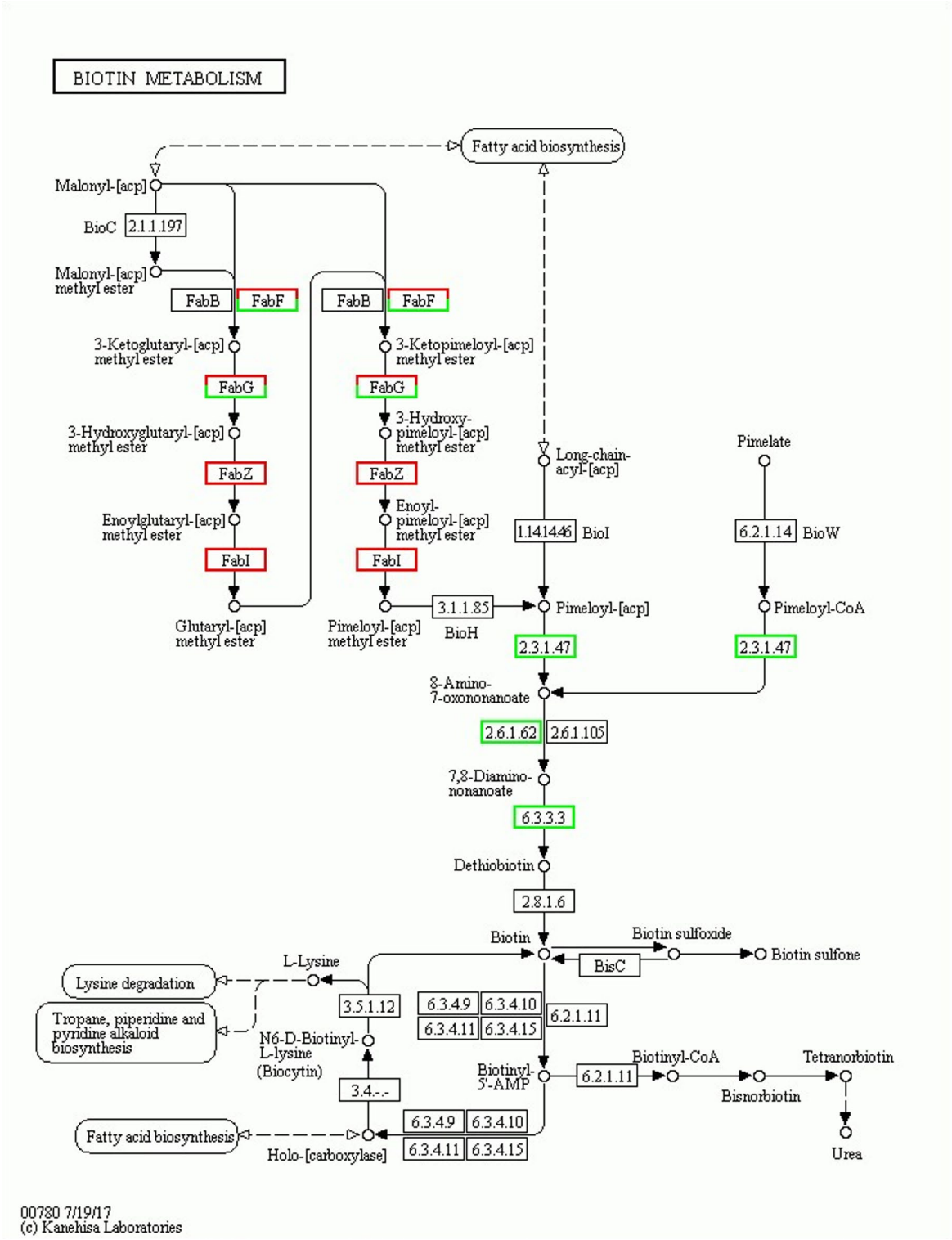

Fig. 10. The gene expression in the pathway of biotin metabolism[26].

metabolic pathway, another defense mechanism, was significantly enriched following mycelium invasion, with numerous enzyme genes in its synthesis pathway being upregulated. Our findings indicate that flavonoid and flavonoid-related metabolic pathways are enriched at SY following mycelial invasion, allowing us to hypothesize some involvement in the symbiotic interaction between *Cr. appendiculata* orchid seeds and *Co. disseminatus* DJF-10.

During the symbiotic interaction between plants and fungi, fungi depend on ectosomes to acquire nutrients from the cell, prompting plants to effectively recognize and bolster their defenses against fungal invasion[23].

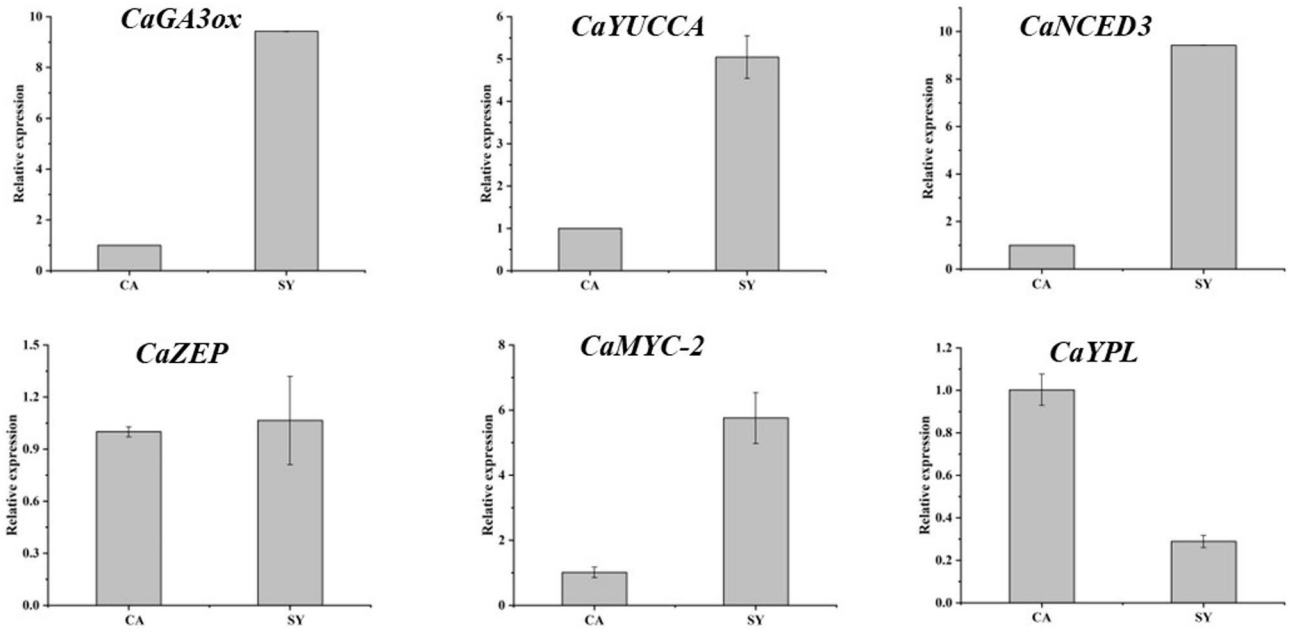

Fig. 11. Relative expression levels of six genes in endogenous hormones of *Cr. appendiculata*.

Mannose-binding lectin proteins play a crucial role in defending against foreign microorganisms and are a vital component of the plant immune system. This study discovered that numerous genes encoding lectin proteins were upregulated in the SY group. Similar observations were reported in *Serapias vomeracea*[16], where lectin proteins were produced in large quantities to inhibit fungal growth before establishing a stable symbiotic relationship with the fungus. Furthermore, lectin proteins are abundantly expressed during the symbiotic germination of orchid seeds, enhancing host resistance by preventing fungal proliferation within host cells. Upon colonization of the embryo's basal cells by *Co. disseminatus* DJF-10 mycelium, the host did not exhibit strong resistance, aligning with the symbiotic interaction mechanisms observed in *Bl. striata*, *Serapias vomeracea*, and *Tulasnella calospora*[4,16]. This suggests a symbiotic germination mechanism between *Cr. appendiculata* and *Co. disseminatus* that is similar to those found in other plant-fungus symbioses. On the fungal side, the symbiotic fungus might release inhibitors to dampen the host's disease resistance response. On the host side, the strategy may involve utilizing saprophytic fungi through signaling pathways rather than mounting a strong stress response[4]. Additionally, calcium-dependent protein kinase (CDPK) plays a significant role in various aspects of plant growth and development[2,4]. Transcriptome data analysis of *Dendrobium officinalis* and *Bl. striata* with mycobionts suggested the involvement of Ca^{2+} signal transduction genes in the interaction between orchids and their symbiotic fungi[2,4]. Our transcriptome data also indicated enrichment of Ca^{2+} signaling pathways, warranting further investigation in future research.

Plant hormones play a crucial role in both seed germination and the successful establishment of symbiotic relationships between hosts and fungi[33]. It is well-known that the antagonism between ABA and GA regulates seed germination. As one of the limiting factors of seed germination, ABA created an unfavorable environment before the lignification of *Cr. appendiculata* seeds, and the synthesis of ABA promoted the embryo to enter a dormant state. During the symbiotic germination between *Cr. appendiculata* and *Co. disseminatus* DJF-10, the seed coat barrier was removed, the seed embryo became breathable and permeable, and seed germination was promoted by the reduction of ABA synthesis[14]. Interestingly, higher JA levels were detected in ungerminated seeds of *Cr. appendiculata* but not in mature seeds of *Dendrobium officinalis*, where JA was only detected post-germination[2]. This pattern mirrors that of *Arabidopsis thaliana*, where mature seeds do not accumulate significant amounts of JA, which only increases notably during germination. However, in rice, ABA has been found to synergistically inhibit seed germination by promoting JA synthesis, suggesting species-specific roles of JA in seed germination regulation[17]. Could the more challenging germination of *Cr. appendiculata* mature seeds, compared to *De. officinalis* and *Bl. striata*, be attributed to the higher content of JA? Further explorations (such as biochemical experiment) are needed to determine whether JA and ABA jointly inhibit seed germination.

Conclusion

Based on the physiological and transcriptomic data analysis, we propose that the interaction between *Cr. appendiculata* seeds during symbiotic germination and its mycobiont *Co. disseminatus* DJF-10 is complex. The mycelium serves as a bridge, transferring water and nutrients, particularly carbon and nitrogen, to the host. Furthermore, the fungus may form pelotons within the embryo cells, which are then degraded to provide nutrients for the host. This study demonstrates that carbohydrate metabolism, glycolysis/gluconeogenesis, fatty acid metabolism, and glutathione metabolism are distinctly influenced in comparisons between CA and SY.

Fungal invasion seems to induce metabolic changes in the host and initiate plant defense responses during the formation of symbiosis between *Cr. appendiculata* and *Co. disseminatus* DJF-10.

Received: 23 March 2025; Accepted: 22 December 2025
Published online: 28 December 2025

References

1. Christenhusz, M. J. M. & Byng, J. W. The number of known plants species in the world and its annual increase. *Phytotaxa* **261** (3), 201–217 (2016).
2. Chen, J. et al. Symbiotic and asymbiotic germination of *Dendrobium officinale* (Orchidaceae) respond differently to exogenous gibberellins. *Int. J. Mol. Sci.* **21**, 6104–6126 (2020).
3. Hoang, N. H., Kane, M. E., Radcliffe, E. N., Zettler, L. W. & Richardson, L. W. Comparative seed germination and seedling development of the ghost orchid, *Dendrophylax Lindenii* (Orchidaceae), and molecular identification of its mycorrhizal fungus from South Florida. *Ann. Bot.* **119** (3), 379–393 (2017).
4. Miura, C. et al. The mycoheterotrophic symbiosis between orchids and mycorrhizal fungi possesses major components shared with mutualistic plant-mycorrhizal symbioses. *Mol. Plant. Microbe Interact.* **31** (10), 1032–1047 (2018).
5. Chen, J., Wang, H., Liu, S. S., Li, Y. Y. & Guo, S. X. Ultrastructure of symbiotic germination of the Orchid *Dendrobium officinale* with its mycobiont *Sebacina Sp*. *Aust J. Bot.* **62** (3), 229–234 (2014).
6. Gao, Y. Y. et al. Mycorrhizal fungus *Coprinellus disseminatus* influences seed germination of the terrestrial Orchid *Cremastra appendiculata* (D. Don. *Makino Sci. Hortic.* **293** (1), 110274–110283 (2022a).
7. Kuga, Y., Sakamoto, N. & Yurimoto, H. Stable isotope cellular imaging reveals that both live and degenerating fungal pelotons transfer carbon and nitrogen to Orchid protocorms. *New. Phytol.* **202** (2), 594–605 (2014).
8. Pierce, S., Spada, A., Caporali, E., Ceriani, R. M. & Buffa, G. Enzymatic scarification of *Anacamptis Morio* (Orchidaceae) seed facilitates lignin degradation, water uptake and germination. *Plant. Biol.* **21** (3), 409–414 (2019).
9. Fang, L. et al. Transcriptome analysis provides insights into the non-methylated lignin synthesis in *Paphiopedilum Armeniacum* seed. *BMC Genom*. **21** (1), 524–538 (2020).
10. Smith, S. E. & Read, D. J. *Mycorrhizal Symbiosis* 3rd edn (Academic, 2008).
11. Valadares, R. B. S., Perotto, S. & Santos, E. C. Proteome changes in *Oncidium sphacelatum* (Orchidaceae) at different trophic stages of symbiotic germination. *Mycorrhiza* **24**, 349–360 (2014).
12. Gebauer, G. & Meyer, M. 15 N and 13 C natural abundance of autotrophic and myco-heterotrophic orchids provides insight into nitrogen and carbon gain from fungal association. *New. Phytol*. **160** (1), 209–223 (2003).
13. Fochi, V. et al. Fungal and plant gene expression in the *Tulasnella calospora-Serapias vomeracea* symbiosis provides clues about nitrogen pathways in Orchid mycorrhizas. *New. Phytol*. **213** (1), 365–379 (2017).
14. Gao, Y. Y., Ji, J., Zhang, Y. J., Yang, N. X. & Zhang, M. S. Biochemical and transcriptomic analyses of the symbiotic interaction between *Cremastra appendiculata* and the mycorrhizal fungus *Coprinellus disseminatus*. *BMC Plant. Biol.* **22** (1), 15–29 (2022b).
15. Chen, J. et al. iTRAQ and RNA-Seq analyses provide new insights into regulation mechanism of symbiotic germination of *Dendrobium officinale* seeds (Orchidaceae). *J. Proteome Res.* **16**, 2174–2187 (2017).
16. Perotto, S. et al. Gene expression in mycorrhizal Orchid protocorms suggests a friendly plant-fungus relationship. *Planta* **239** (6), 1337–1349 (2014).
17. Wang, T. et al. Functional insights into the roles of hormones in the *Dendrobium officinale-Tulasnella sp*. germinated seed symbiotic association. *Int. J. Mol. Sci.* **19** (11), 3484–3499 (2018).
18. Chung, M. Y. et al. Population history of the terrestrial Orchid *Cremastra appendiculata* var. Variabilis from Korea, inferred from levels and distribution of genetic diversity. *Bot. J. Linn. Soc.* **173**, 721–732 (2013).
19. Lee, Y., Chung, M., Yeung, E. C. & Lee, N. Dynamic distribution and the role of abscisic acid during seed development of a lady's slipper orchid, *Cypripedium formosanum*. *Ann. Bot.* **116**, 403–411 (2015).
20. Li, H. et al. The effect of 1-methylcyclopropene, Methyl jasmonate and Methyl salicylate on lignin accumulation and gene expression in postharvest Xuxiang Kiwifruit during cold storage. *Postharvest Biol. Tec.* **124**, 107–118 (2017).
21. Langmead, B. & Salzberg, S. L. Fast gapped-read alignment with bowtie 2. *Nat. Methods*. **9** (4), 357–359 (2012).
22. Grabherr, M. G. et al. Full-length transcriptome assembly from RNA-Seq data without a reference genome. *Nat. Biotechnol.* **29** (7), 644–652 (2011).
23. Zeng, X. et al. Transcriptomic analyses reveal clathrin-mediated endocytosis involved in symbiotic seed germination of *Gastrodia Elata*. *Bot. Stud.* **58** (1), 31–41 (2017).
24. Uetake, Y., Kobayashi, K. & Ogoshi, A. Ultrastructural changes during the symbiotic development of *Spiranthes sinensis* (Orchidaceae) protocorms associated with binucleate *Rhizoctonia* anastomosis group C. *Mycol. Res.* **96** (3), 199–209 (1992).
25. Megha, S., Wang, Z., Kav, N. V. V. & Rahman, H. Genomep-wide identification of biotin carboxyl carrier subunits of acetyl-CoA carboxylase in brassica and their role in stress tolerance in oilseed *Brassica Napus*. *BMC Genomics*. **23**, 707–729 (2022).
26. Kanehisa, M. & Goto, S. K. E. G. G. Kyoto encyclopedia of genes and genomes. *Nucleic Acids Res.* **28**, 27–30 (2000).
27. León, D. R. Biotin in metabolism, gene expression, and human disease. *J. Inherit. Metab. Dis.* **42** (4), 647–654 (2019).
28. Cameron, D. D., Leake, J. R. & Read, D. J. Mutualistic mycorrhiza in Orchids: evidence from plant-fungus carbon and nitrogen transfers in the green-leaved terrestrial Orchid *Goodyera repens*. *New. Phytol*. **171** (2), 405–416 (2006).
29. Barsberg, S. T., Lee, Y. I. & Rasmussen, H. N. Development of Clignin with G/Slignin and lipids in Orchid seed coats-an unexpected diversity exposed by ATRFTIR spectroscopy. *Seed Sci. Res.* **28**, 41–51 (2018).
30. Yagame, T., Funabiki, E., Nagasawa, E., Fukiharu, T. & Iwase, K. Identification and symbiotic ability of *Psathyrellaceae* fungi isolated from a photosynthetic orchid, *Cremastra appendiculata* (Orchidaceae). *Am. J. Bot.* **100** (9), 1823–1830 (2013).
31. Blakeman, J. P., Mokahel, M. A. & Hardley, G. Effect of mycorrhizal infection on respiration and activity of some oxidase enzymes of Orchid protocorms. *New. Phytol*. **77**, 697–704 (1976).
32. Marta, B., Szafrańska, K. & Posmyk, M. Exogenous melatonin improves antioxidant defense in cucumber seeds (*Cucumis sativus* L.) germinated under chilling stress. *Front. Plant. Sci.* **7**, 575–586 (2016).
33. Foo, E., Plett, J. M., Lopez-Raez, J. A., Reid, D. & Editorial The role of plant hormones in plant-microbe symbioses. *Front. Plant. Sci.* **10**, 1391–1393 (2019).

Acknowledgements

The datasets generated during the current study are available from the corresponding author upon reasonable request (accession No. PRJNA1065130).

Author contributions

Yanyan Gao methodology, designed, analyzed and wrote the manuscript. Huang Lei designed the research work. Both authors read and approved the final manuscript.

Funding
This work was supported by the National Natural Science Foundation of China (NO. 32360078), Guizhou Provincial Basic Research Program (Natural Science) (NO. Qiankehe-zk[2025]566), the Guizhou Administration of Traditional Chinese Medicine (GZZY-2025-076), the Doctoral Scientific Research Foundation of Guizhou Medical University (No. [2022]068), the National Natural Science Foundation of China Cultivation Project of Guizhou Medical University (NO. 22NSFCP16).

Declarations

Competing interests
The authors declare no competing interests.

Additional information
Supplementary Information The online version contains supplementary material available at https://doi.org/10.1038/s41598-025-33845-3.

Correspondence and requests for materials should be addressed to Y.G.

Reprints and permissions information is available at www.nature.com/reprints.

Publisher's note Springer Nature remains neutral with regard to jurisdictional claims in published maps and institutional affiliations.